PHYSICAL REVIEW B VOLUME 47, NUMBER 17 1 MAY 1993-I

Cobalt site preferences in iron rare-earth-based compounds

L. X. Liao,* Z. Altounian, and D. H. Ryan
Centre for the Physics of Materials and Department of Physics, McGill University, 3600 University Street, Montréal, Québec, Canada H3A 2T8

(Received 12 October 1992; revised manuscript received 12 January 1993)

A systematic study of cobalt site preferences has been carried out in a number of rare-earth iron compounds. The Mössbauer source technique employed in this work offers a direct and unambiguous way to determine quantitatively cobalt site preferences in these compounds at extremely low cobalt contents. Data quality as well as counting efficiency for the source (^{57}Co doped) samples is improved by using a resonant-conversion-electron detector. Our results have produced convincing evidence that cobalt substitutes preferentially for iron in all of the compounds investigated. We find that the site volume is the dominant factor controlling preferential cobalt substitutions at transition-metal sites with volume < 12.2 Å^3. The cobalt preference for a site decreases linearly with increasing site volume at a rate of ~ 0.9 Å^{-3}. In general, cobalt shows a preference for sites with a volume greater than 11.8 Å^3. As the site volume becomes sufficiently large (≥ 12.2 Å^3), the negative enthalpy of mixing between cobalt and rare earth plays a significant role and leads cobalt to prefer sites with the highest number of rare-earth nearest neighbors.

I. INTRODUCTION

The recent discovery of the ternary rare-earth-iron-boron compound, $R_2Fe_{14}B$ (R = rare-earth atom),[1,2] has renewed worldwide research on iron-based rare-earth hard magnetic materials. The coercive forces as well as Curie temperature ($T_c = 585$ K) attainable in Nd-Fe-B materials are relatively low, and many efforts have been made to improve the performance of $Nd_2Fe_{14}B$-based hard magnetic materials. Studies on $R_2Fe_{14}B$ with nonmagnetic rare earths such as Y and La have demonstrated that the magnetism of the $R_2Fe_{14}B$ compounds originates mainly from the Fe sublattice.[3,4] One expects, therefore, that Fe replacements will have significant effects on the magnetic properties of $Nd_2Fe_{14}B$-based magnet materials. It has been found that cobalt is capable of replacing iron over the whole concentration range, while maintaining the integrity of the crystal structure. Fuerst, Herbst, and Alson[5] have shown that the T_c of $Nd_2Fe_{14-x}Co_xB$ increases with increasing Co concentration, the increase in T_c being most rapid at the lowest Co concentrations. Furthermore, the room temperature saturation magnetization of $Nd_2Fe_{14-x}Co_xB$ features a modest maximum in the vicinity of $x = 2$. In order to understand or predict the effects of cobalt substitutions on the magnetic properties of $Nd_2(Fe_{1-x}Co_x)_{14}B$ and other iron-based rare-earth magnetic materials, it is necessary to know how the cobalt atoms are distributed among the various crystallographically inequivalent iron sites.

The earliest work on Co site preferences reported by van Diepen, Buschow, and van Wieringen[6] (1972) and Laforest and Shaw[7] (1973) was one on $Th(Fe_{1-x}Co_x)_5$ alloys, whose crystal structure contains two crystallographically distinct transition-metal sites in the ratio 3:2 (Wyckoff notation 3g and 2c). Neutron diffraction and standard transmission Mössbauer spectroscopy showed that Co substitution in these alloys does not occur statistically on the two available sites. The results obtained by these two techniques, however, were contradictory. Neutron diffraction[7,8] found an excess Co occupations of the 2c site, whereas the results of the Mössbauer measurements suggested a Co avoidance of this site. Since then, studies on site preferences have been extended to other Co substituted binary R-Fe compounds such as R_2Fe_{17} and RFe_3,[9–11] and more recently to the ternary compound $R_2Fe_{14}B$.[12–14]

The techniques involved in previous studies on Co-site preferences in Fe-based rare-earth compounds are mainly neutron diffraction, standard Mössbauer spectroscopy, and nuclear magnetic resonance (NMR). Neutron-diffraction studies[9,10,12,15,16] exploit the differences between neutron-nuclear coherent scattering length b ($b_{Fe} = 0.95 \times 10^{-14}$m, $b_{Co} = 0.28 \times 10^{-14}$ m) to determine the site preferences in Co substituted iron-based compounds. Besides the usual adjustable magnetic and nuclear parameters needed to fit the data, additional parameters for the Co nuclear positions and site-occupation numbers are included in the refinements for the Co-substituted alloys. The Co-site occupations are deduced from the changes in average scattering length of the calculated diffraction patterns. It should be pointed out that in order to observe a clear site preference, relatively high cobalt concentrations have to be used.

Both Mössbauer and NMR studies use the ^{57}Fe nucleus as local probes of the magnetic properties of the iron sites. In the standard ^{57}Fe Mössbauer studies, the determination of Co-site occupations is similar to that used in neutron diffraction, i.e., Co-site preferences are deduced from the changes in the iron signal. The deviation of Co occupations from a random distribution is determined from the fitted spectra, which include the additional parameter of Fe occupation for each subspec-

trum as the relative intensities of the subspectra are no longer constrained. This technique, similar to neutron diffraction, also requires relative high Co content in order to see significant changes in spectrum. With increasing Co concentrations, however, the hyperfine fields of the spectra are reduced and the lines are broadened because of the distribution of substituting atoms on near-neighbor sites. These effects greatly reduce the resolution of the spectrum and lead to large uncertainties in the results of the fitting.

In ^{57}Fe NMR spectroscopy, the NMR spectrum is a distribution of hyperfine fields on the crystallographically distinct iron sites as a function of frequency. The ^{57}Fe NMR resonant frequency is slightly different at each inequivalent iron site because of differences in local atomic environments. The effect of Co substitutions on the spectra is seen as a peak shift towards lower frequencies, which is an indication of a reduction in the hyperfine field at the Fe nucleus. The evidence for Co selectivity is obtained from the analysis of these ^{57}Fe line shifts and relative intensity changes in the ^{57}Fe NMR spectrum as well as the effects of Co addition on the local field at other nu-

TABLE I. Crystallographic data for R-Fe compounds. Included are structure type, lattice constants, space group, atomic sites (multiplicity and Wyckoff notation), and nuclear coordinates x,y,z (in units of the lattice constants) (Refs. 15 and 41).

Compound	Structure type and lattice constants (Å)	Space group	Atom	Point symmetry	Atomic positions
$Nd_2Fe_{14}B$	Tetragonal	$P4_2/mnm$	Fe(4*e*)	*mm*	(0.500,0.500,0.114)
	$Nd_2Fe_{14}B$	No. 136	Fe(4*c*)	2/*m*	(0.000,0.500,0.000)
	$a=8.800$		Fe($8j_1$)	*m*	(0.098,0.098,0.204)
	$c=12.200$		Fe($8j_2$)	*m*	(0.317,0.317,0.246)
			Fe($16k_1$)	1	(0.223,0.567,0.127)
			Fe($16k_2$)	1	(0.037,0.360,0.176)
			Nd(4*f*)	*mm*	(0.268,0.268,0.000)
			Nd(4*g*)	*mm*	(0.140,−0.140,0.00)
			B(4*g*)	*mm*	(0.371,−0.371,0.00)
Nd_2Fe_{17}	Rhombohedral	$R\bar{3}m$	Fe(6*c*)	3*m*	(0.000,0.000,0.096)
	Th_2Zn_{17}	No. 166	Fe(9*d*)	2/*m*	(0.500,0.000,0.500)
	$a=8.578$		Fe(18*f*)	2	(0.286,0.000,0.000)
	$c=12.462$		Fe(18*h*)	*m*	(0.500,0.500,0.148)
			Nd(6*c*)	3*m*	(0.000,0.000,0.333)
Gd_2Fe_{17}	Hexagonal	$P6_3/mmc$	Fe(4*f*)	3*m*	(0.333,0.667,0.105)
	$Ni_{17}Th_2$	No. 194	Fe(6*g*)	2/*m*	(0.500,0.000,0.000)
	$a=8.496$		Fe(12*j*)	*m*	(0.333,0.969,0.250)
	$c=8.345$		Fe(12*k*)	*m*	(0.167,0.333,0.985)
			Gd(2*b*)	$\bar{6}m2$	(0.000,0.000,0.250)
			Gd(2*d*)	$\bar{6}m2$	(0.333,0.667,0.750)
Dy_2Fe_{17}	Hexagonal	$P6_3/mmc$	Fe(4*f*)	3*m*	(0.333,0.667,0.105)
	$Ni_{17}Th_2$	No. 194	Fe(6*g*)	2/*m*	(0.500,0.000,0.000)
	$a=8.448$		Fe(12*j*)	*m*	(0.333,0.969,0.250)
	$c=8.295$		Fe(12*k*)	*m*	(0.167,0.333,0.985)
			Dy(2*b*)	$\bar{6}m2$	(0.000,0.000,0.250)
			Dy(2*d*)	$\bar{6}m2$	(0.333,0.667,0.750)
$ThFe_5$	Hexagonal	$P6/mmm$	Fe(2*c*)	$\bar{6}m2$	(0.333,0.667,0.000)
	$CaCu_5$	No. 191	Fe(3*g*)	*mmm*	(0.500,0.000,0.500)
	$a=5.116$		Th(1*a*)	6/*mmm*	(0.000,0.000,0.000)
	$c=4.046$				
Er_6Fe_{23}	Cubic	$Fm\bar{3}m$	Fe(4*b*)	$m3m$	(0.500,0.500,0.500)
	Th_6Mn_{23}	No. 225	Fe(24*d*)	*mmm*	(0.000,0.250,0.250)
	$a=12.005$		Fe($32f_1$)	3*m*	(0.178,0.178,0.178)
			Fe($32f_2$)	3*m*	(0.378,0.378,0.378)
			Er(24*e*)	4*mm*	(0.203,0.000,0.000)
$DyFe_3$	Rhombohedral	$R\bar{3}m$	Fe(3*b*)	$\bar{3}m$	(0.000,0.000,0.500)
	$PuNi_3$	No. 166	Fe(6*c*)	3*m*	(0.000,0.000,0.334)
	$a=5.123$		Fe(18*h*)	*m*	(0.500,0.500,0.083)
	$c=24.570$		Dy(3*a*)	$\bar{3}m$	(0.000,0.000,0.000)
			Dy(6*c*)	3*m*	(0.000,0.000,0.141)

clei such as ^{10}B.[14] In comparison with neutron diffraction and standard Mössbauer spectroscopy, NMR is much more indirect and less suitable for studies on site preference.

Co-site preferences in $R_2Fe_{14}B$ have been explored by neutron diffraction,[12] standard Mössbauer spectroscopy,[13,17–23] and nuclear magnetic resonance (NMR).[14,24,25] Although there is almost unanimous agreement among the studies conducted that Co strongly avoids the $8j_2$ site, the results for the other five sites are conflicting and add nothing but confusion to the question of the effects of Co substitutions on the magnetic properties of $Nd_2Fe_{14}B$. Other conflicting results regarding Co substitutions are also found in Co-substituted binary R-Fe compounds, especially R_2Fe_{17}.[9,10,16,26,27] The confusion stems from the fact that the identification of the cobalt location is indirect as it can only be deduced from a reduction in the iron signal.

The Mössbauer source technique used in this work allows direct measurement of cobalt locations, and uses a single Co-doped alloy at extremely low cobalt content (~ 1 ppm), which is, therefore, virtually indistinguishable from the reference (cobalt-free) material.[28] In this technique, the radioactive ^{57}Co is incorporated into the sample (prepared with the isotope ^{56}Fe rather than natural iron to prevent loss of the signal from resonant self-absorption by the ^{57}Fe present in natural iron), where it decays by electron capture with a half life of 270 days to an excited state of ^{57}Fe. This subsequently passes to its ground state thereby emitting the 14.4 keV γ ray that can be used in a standard transmission Mössbauer experiment. The complex emission pattern is analyzed using a single-line absorber such as 310 stainless steel foil. The signal comes from ^{57}Fe nuclei in a virtually pure (i.e., cobalt-free) alloy, and the observed subspectra are identical to those of a standard sample with no disorder-induced line broadening. However, the Fe atoms that emit the radiation are in sites occupied before the electron capture event and thus chosen by cobalt atoms. Thus, only the sites actually occupied by cobalt atoms contribute to the Mössbauer spectrum.

In general, a Co-free sample, serving as a reference, is measured to obtain the best hyperfine parameters for the observed spectrum. These parameters are then used to fit the spectrum of the source sample with only the intensities of the individual subspectra as adjustable parameters (in addition to the off-resonance baseline and linewidth). Requiring both the reference and source spectra to be fitted by the same hyperfine parameters, with changes only in the subspectrum intensities for the source spectrum, imposes a very severe constraint on the fit and provides a consistency check on the parameters used for the reference spectrum. Furthermore, with low doping levels, Co substitutions are not influenced by Co-Co interactions.

We present here a systematic study of cobalt-site preferences in all of the equilibrium iron-based binary rare-earth intermetallic compounds. The particular compounds selected for study are Nd_2Fe_{17}, Gd_2Fe_{17}, Dy_2Fe_{17}, Er_6Fe_{23}, $DyFe_3$, and $ThFe_5$. In view of the possible effect of structural differences on Co-site preference, three R_2Fe_{17} compounds have been included in this study as these compounds exist in two closely related structural modifications: hexagonal ($P6_3/mmc$) and rhombohedral ($R\bar{3}m$). Alloys of Nd_2Fe_{17} and Dy_2Fe_{17} have the rhombohedral and hexagonal structures respectively, while Gd_2Fe_{17} could have either structure type. Although thorium is not a rare earth, the compound $ThFe_5$ was included in the study as it is the only example of the hexagonal $CaCu_5$ structure known to occur with iron. Both the hexagonal and rhombohedral R_2Fe_{17} structures and the RFe_3 structure originate from the $CaCu_5$ lattice and may be derived from it through some simple substitutions accompanied by layer shifts.[29] Furthermore, with only two crystallographically inequivalent iron sites, $ThFe_5$ is the simplest compound in which site preferences could be observed. $Nd_2Fe_{14}B$ was also studied because of its technological importance as a permanent magnet material and to evaluate the considerable amounts of conflicting data on Co-site preferences in this compound. The compounds selected represent a variety of crystal structures and provide a large number of crystallographic sites with various symmetries and local environments. The crystallographic data of the various compounds investigated are summarized in Table I.

II. EXPERIMENTAL METHODS

Reference samples (*cobalt free*) were obtained by rf-induction melting appropriate amounts of 99.9% pure elements on a water-cooled copper boat under Ti-gettered argon. To ensure homogeneity, all samples were melted up to five times. As-made ingots wrapped in Ta foil were sealed into quartz tubes evacuated to $\sim 10^{-6}$ mbar and annealed for about 2 weeks at 1173 K or higher. The annealing treatment is essential for preparing single-phase alloys of Nd_2Fe_{17} and $ThFe_5$. In the case of Nd_2Fe_{17}, the as-made alloys contained a large amount of α-Fe. After heat treatment, essentially α-Fe-free Nd_2Fe_{17} alloys were obtained. For $ThFe_5$ alloys, the as-made ingots were found to contain mainly the Th_2Fe_{17}, $ThFe_3$, and Th_2Fe_7 phases with only a small fraction of $ThFe_5$ present. Samples with a majority of the $ThFe_5$ phase were obtained only after annealing at about 1430 K for 2 weeks followed by quenching in water.[30]

Source samples (^{57}Co doped) were prepared by incorporating the radioisotope ^{57}Co (~ 1 ppm) into iron metal prior to alloying with the other elements. 37-MBq ^{57}Co is supplied as cobalt chloride ($^{57}CoCl_2$) in 0.5-M hydrochloric acid (HCl) by New England Nuclear Medical Products.[31] $^{57}CoCl_2$ was neutralized with NH_4OH and evaporated to dryness in an oven at about 80 °C. ^{57}Co, deposited in the bottom of the container, was then mixed with ~ 150 mg of $^{56}Fe_2O_3$ (corresponding to about 100-mg ^{56}Fe). Here ^{56}Fe rather than natural iron is used to prevent loss of signal from resonant self-absorption by the 2.17 at. % ^{57}Fe present in natural iron. A few drops of distilled water were added into the container to form a uniform mixture of ^{57}Co and $^{56}Fe_2O_3$. Once again, the mixture was dried at about 80 °C in the oven. The ma-

terial was then transferred into a Ni boat and reduced to the metallic state by annealing at 900 °C under flowing H_2 for about 2 h. Finally, the radioactive iron metal (containing ~27 MBq ^{57}Co) and appropriate amounts of the other elements were pressed into a pellet with a typical mass of ~150 mg. Small samples were prepared because the limited range of the 14.4-keV γ ray requires the use of thin sources (about 50-mg samples were used in the measurements). The small pellet was melted under argon in a specially constructed miniature rf-induction melter. The as-made ingots were annealed under the same conditions as their corresponding reference samples.

All of the samples were examined by x-ray diffraction using an automated Nicolet-Stöe L11 powder diffractometer with Cu$K\alpha$ radiation ($\lambda = 1.5418$ Å). Some examples of x-ray-diffraction patterns for R_2Fe_{17} are shown in Fig. 1. The results confirm the single-phase nature and rhombohedral (Nd_2Fe_{17}) and hexagonal (Gd_2Fe_{17} and Dy_2Fe_{17}) structures. Thermomagnetic measurements were performed using a Perkin-Elmer thermogravimetric analyser (TGA-7) in a small field gradient. Figure 2 shows TGA scans for as-made and annealed samples of $ThFe_5$. The multiphase nature of the as-made sample for $ThFe_5$, clearly seen in Fig. 2(b), is reduced to $ThFe_5$ and Th_2Fe_{17} phases after annealing as shown in Fig. 2(a).

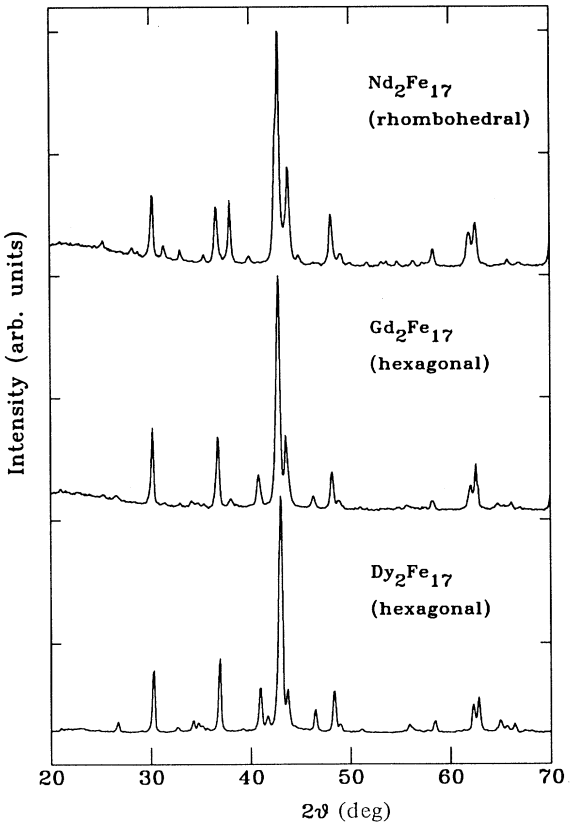

FIG. 1. X-ray diffraction patterns for the reference samples of R_2Fe_{17} (R = Nd,Gd,Dy).

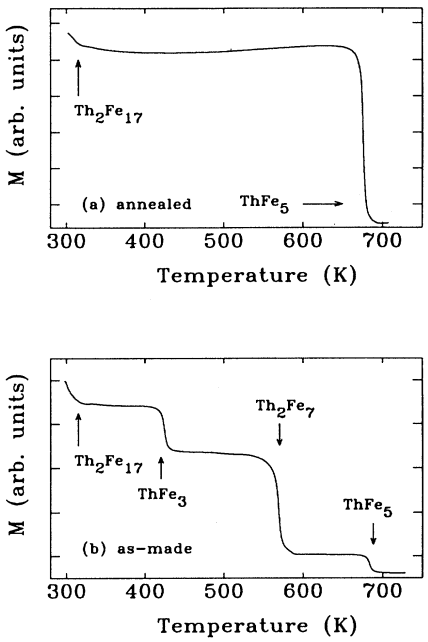

FIG. 2. TGA scans for as-made and annealed reference samples of $ThFe_5$. The multiphase nature of the as-made sample is clearly seen from the TGA curve shown in (b).

The Mössbauer spectra for reference samples were obtained in the standard transmission geometry with a 1-GBq ^{57}CoRh single-line source on a constant acceleration spectrometer. A Dewar with a cold finger was used to obtain spectra at liquid-nitrogen temperature (77 K). The reference spectra were fitted using a standard nonlinear least-squares minimization routine with subspectra intensities constrained to match crystallographic multiplicities. Best fit parameters are given in Table II.

For the Mössbauer source measurements, we constructed a resonant conversion electron detector with a mass of ~25 g, utilizing 90% ^{57}Fe-enriched stainless-steel foil. This lightweight detector not only allows low-temperature source measurements to be made, but also yields a more than six-fold enhancement in signal-to-noise ratio over conventional transmission methods. A detailed description of this detector has been published elsewhere.[32] All of the source spectra were obtained using this conversion electron detector. The typical counting time for each spectrum is about two weeks. When Mössbauer measurements at a reduced temperature were required, the detector, rather than the source, was mounted on the Mössbauer drive and the source sample was placed in the cryostat. All source spectra were simply fitted using the best-fit parameters obtained from the reference spectra by allowing only the off-resonance baseline, linewidth, and intensities of the individual subspectra to vary. Source spectra linewidths were, in general, less than 0.01 mms^{-1} greater than the corresponding reference spectra, with the broadening being due to geometrical effects resulting from the short source-detector separations employed.

III. RESULTS

A. $Nd_2Fe_{14}B$

X-ray-diffraction and TGA results confirm that both the reference and source samples of $Nd_2Fe_{14}B$ consist of tetragonal $P4_2/mnm$-phase $Nd_2Fe_{14}B$. The reference sample contained $\sim 2\%$ $Nd_{1.1}Fe_4B_4$. No impurity phase was detected in the source sample. The room-temperature Mössbauer spectrum of the reference sample for $Nd_2Fe_{14}B$, shown in Fig. 3, was fitted with six subspectra in the ratio 16:16:8:8:4:4 corresponding to the multiplicities of the k_1, k_2, j_1, j_2, c, and e sites, respectively. More details of the fitting are given in Ref. 28. The fit is shown in Fig. 3 as the solid line through the data points. If the cobalt simply substituted randomly for iron in the structure then the source spectrum would look exactly the same as that of the reference sample.

TABLE II. Summary of fitted parameters [including isomer shift (δ), quadrupole splitting (Δ) and hyperfine field (B_{hf}) and linewidth (Γ) half width at half maximum] for the reference spectra of R_2Fe_{17} (R =Nd,Gd,Dy), $DyFe_3$, and $ThFe_5$. All spectra were obtained at room temperature except for those of Nd_2Fe_{17} and Dy_2Fe_{17}, which were measured at 77 K. Isomer shifts are given relative to α-Fe at room temperature.

Compound	Site	Occupation	δ (mm/s)	Δ (mm/s)	B_{hf} (T)	Γ (mm/s)
$Nd_2Fe_{14}B$	e	1	0.01(1)	−0.78	28.8(1)	0.158
	c	1	−0.07	0.07	25.6	
	j_1	2	−0.04	0.29	27.9	
	j_2	2	0.10	0.65	34.3	
	k_1	4	−0.01	0.26	28.8	
	k_2	4	−0.09	0.17	30.6	
Nd_2Fe_{17}	h	4	0.06(1)	−0.29(2)	26.6(1)	0.160
		2	0.06	0.42	27.8	
	f	4	0.00	−0.07	31.0	
		2	0.00	0.58	27.2	
	d	3	−0.08	0.12	28.2	
	c	2	0.22	0.05	34.7	
Gd_2Fe_{17}	k	4	−0.15(2)	−0.16(2)	23.5(1)	0.154
		2	−0.15	0.48	22.9	
	j	2	−0.09	−0.43	26.5	
		2	−0.09	0.07	26.7	
		2	−0.09	−0.04	21.2	
	g	2	−0.11	0.09	25.6	
		1	−0.11	0.30	23.9	
	f	2	0.06	0.05	30.2	
Dy_2Fe_{17}	k	4	0.02(1)	0.16(2)	31.1(1)	0.160
		2	0.02	−0.26	26.3	
	j	2	0.05	0.42	26.8	
		2	0.05	0.25	27.0	
		2	0.05	−0.41	32.2	
	g	2	−0.07	−0.03	30.6	
		1	−0.07	0.27	29.1	
	f	2	0.20	0.07	36.1	
Er_6Fe_{23}	f_1	6	−0.16(1)	−0.04(2)	21.6(1)	0.154
		2	−0.16	0.13	20.8	
	f_2	6	0.01	0.13	26.6	
		2	0.01	−0.34	26.5	
	d	4	−0.14	0.03	23.8	
		2	−0.14	0.00	22.9	
	b	1	−0.03	0.03	30.8	
$DyFe_3$	h	2	−0.14(2)	0.33(2)	21.6(1)	0.152
		2	−0.14	−0.444	20.9	
		2	−0.14	0.06	21.4	
	c	2	−0.11	0.46	22.5	
	b	1	−0.07	0.40	21.4	
$ThFe_5$	c	2	−0.10(2)	0.48(2)	19.7(1)	0.160
	g	1	−0.08	−0.40	21.6	
		1	−0.08	−0.08	24.4	
		1	−0.08	0.40	22.2	

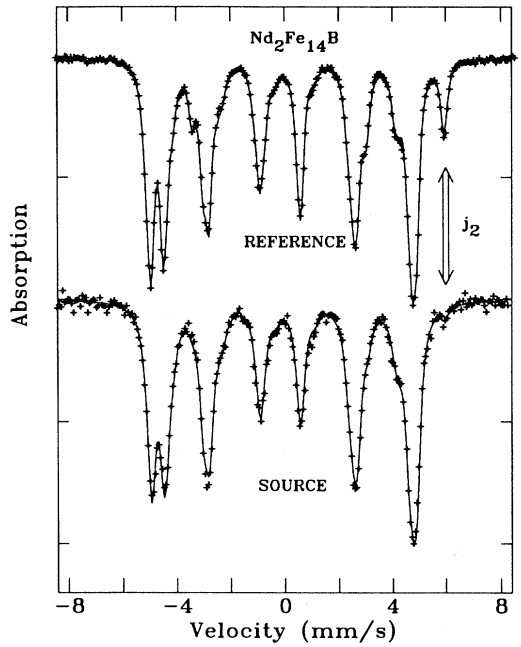

FIG. 3. Mössbauer spectra for the $Nd_2Fe_{14}B$ reference and source samples at room temperature. The source spectrum has been inverted. Arrows indicate the position of the $8j_2$ peak at $6mm/s$, which is absent from the source spectrum.

Clearly this is not the case as we can see from the Fig. 3, where the spectrum of source sample for $Nd_3Fe_{14}B$ is also shown. The source spectrum has been inverted in order to facilitate comparison with the reference spectrum. A visual inspection of Fig. 3 immediately shows that cobalt substitutes preferentially on certain sites. The most obvious difference is that the line at $+6mms^{-1}$, due to the j_2 site, is almost entirely absent from the source spectrum, indicating a strong Co avoidance of this site. The results of the computer fit are summarized in Fig. 4(a), which shows the percent deviations of Co occupations from a random distribution on the six crystallographically inequivalent iron sites. These results clearly indicate the preference of cobalt for the six sites in $Nd_2Fe_{14}B$. It confirms that the $8j_2$ site is strongly avoided, that Co prefers the $8j_1$ and $16k_2$ sites, and shows a small avoidance of the $4c$ site, while populating the remaining $16k_1$ and $4e$ essentially at random.

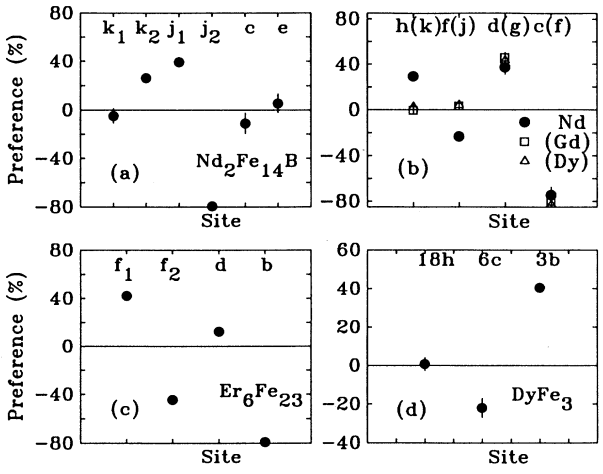

FIG. 4. The deviation (%) of fitted Co-site occupations from a random distribution for the source samples of (a) $Nd_2Fe_{14}B$, (b) R_2 Fe^{17} (R =Nd,Gd,Dy), (c) Er_6Fe_{23}, and (d) $DyFe_3$.

B. R_2Fe_{17} (R =Nd, Gd, Dy)

X-ray diffraction confirmed that the alloys of Gd_2Fe_{17} and Dy_2Fe_{17} had the hexagonal Th_2Ni_{17} ($P6_3/mmc$)-type structure and those of Nd_2Fe_{17} had the rhombohedral Th_2Zn_{17} ($R\bar{3}m$)-type structure. Both x-ray and TGA measurements showed that all of the samples were single phased except for the source samples of Gd_2Fe_{17} and Dy_2Fe_{17}, which contained a few percent of α-Fe. The measured values of Curie temperatures for Nd_2Fe_{17}, Gd_2Fe_{17}, and Dy_2Fe_{17} are 343 K, 486 K, and 400 K, respectively. The Mössbauer spectra for the reference samples of R_2Fe_{17} (R =Nd, Gd, Dy) are shown in Figs. 5–7. The spectrum of Gd_2Fe_{17} was measured at room temperature, while the spectra of Nd_2Fe_{17} and Dy_2Fe_{17} were taken at liquid-nitrogen temperature (77 K), since their low-T_c leads to insufficient resolution of the subspectra at room temperature. The reference spectra of R_2Fe_{17} (R =Nd, Gd, Dy) were fitted with four subspectra in the intensity ratio 2:3:6:6 corresponding to the occupations of the iron sites $6c(4f)$:$9d(6g)$;$18f(12j)$:$18h(12k)$, respectively. The site notations are given for the rhombohedral structure, with corresponding hexagonal nota-

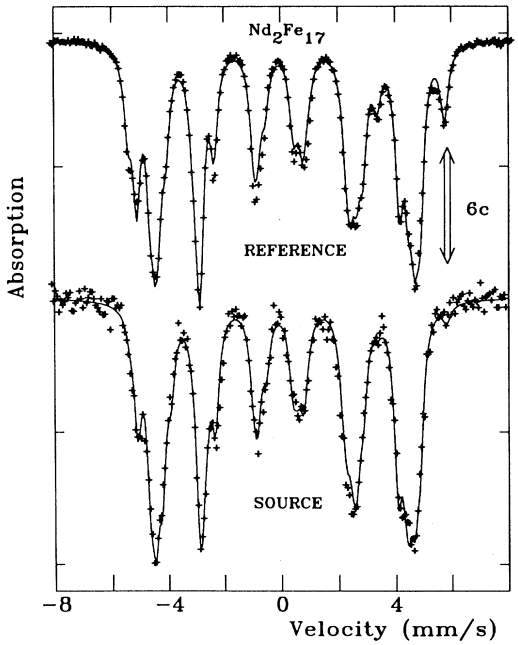

FIG. 5. Mössbauer spectra of the Nd_2Fe_{17} reference and source samples at 77 K. The fits to the data are shown as solid lines. The source spectrum has been inverted. Arrows indicate the position of the $6c$ peak at ~ 5.8 mm/s, which is absent from the source spectrum.

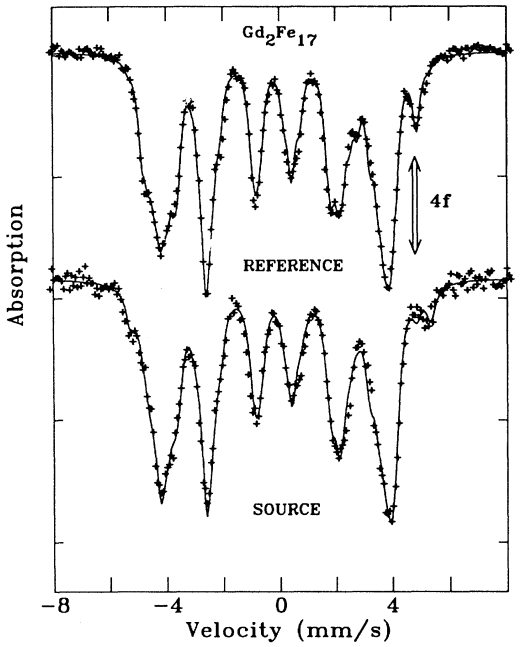

FIG. 6. Mössbauer spectra of the Gd_2Fe_{17} reference and source samples at room temperature. The fits to the data are shown as solid lines. The source spectrum has been inverted. Arrows indicate the position of the $4f$ peak at ~ 4.7 mm/s, which is absent from the source spectrum.

tion in parentheses. To take account of the magnetic easy direction being in the basal plane, we have included a 1:2 magnetic subsplitting of the $18f$ and $18h$ sites for Nd_2Fe_{17},[33] a 1:2 subsplitting for the $(6g)$ and $(12k)$ sites, and a 1:1:1 subsplitting for the $(12j)$ site for Gd_2Fe_{17} and Dy_2Fe_{17}.[26] The hyperfine parameters obtained from the best fit are given in Table II. Figures 5–7 show a comparison between the spectrum of the reference sample and that of the source sample for each of the three compounds. The fits to the data are shown as solid lines in these figures. A common feature observed in these figures is the absence of the outermost line at positive velocity (indicated by the arrows) from all source spectra, indicating almost total Co avoidance of this site $[6c(4f)]$. The results for Co-site preferences obtained from the fits are given in Fig. 4(b). It is interesting to note that identical Co-site preferences are observed for the $6c(4f)$ and $9d(6g)$ sites in both the rhombohedral and hexagonal R_2Fe_{17} structures. Cobalt, while it preferentially occupies the $9d(6g)$ site, almost entirely avoids the dumbbell $[6c(4f)]$ site. The Co preferences in the other two sites, however, exhibit marked differences between the two structures. In rhombohedral Nd_2Fe_{17}, Co shows a clear preference for the $18f$ and $18h$ sites, whereas in the two hexagonal samples it populates the corresponding $(12j)$ and $(12k)$ sites essentially at random. The fact that similar results are obtained for Gd_2Fe_{17} and Dy_2Fe_{17} is consistent with the assumption that, for a given structure, the type of rare-earth atom does not significantly affect the Co-site preferences on the iron sites.

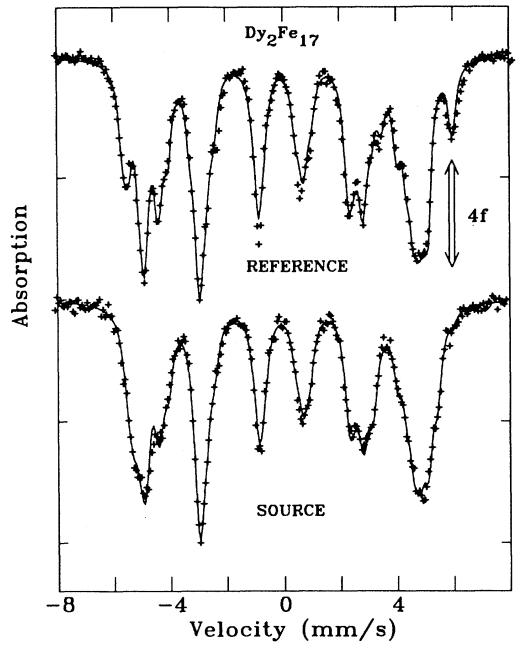

FIG. 7 Mössbauer spectra of the Dy_2Fe_{17} reference and source samples at 77 K. The fits to the data are shown as solid lines. The source spectrum has been inverted. Arrows indicate the position of the $4f$ peak at ~ 6 mm/s, which is absent from the source spectrum.

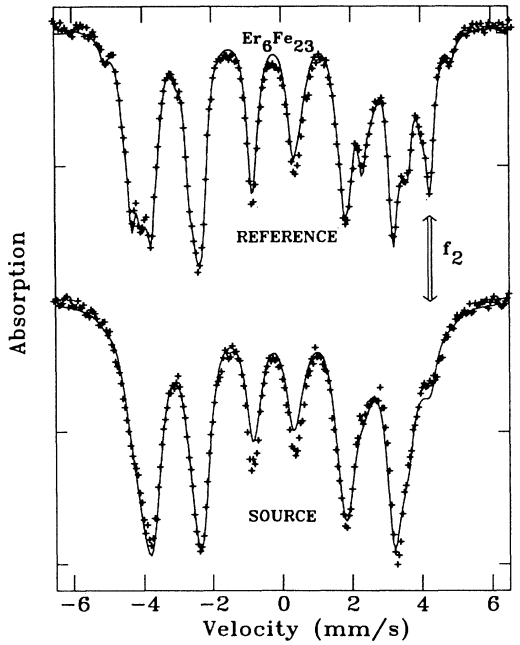

FIG. 8. Mössbauer spectra of the Er_6Fe_{23} reference and source samples at room temperature. The fits of the data are shown as solid lines. The source spectrum has been inverted. Arrows indicate the position of the f_2 peak at ~ 4.2 mm/s, which is greatly reduced in the source spectrum.

C. Er_6Fe_{23}

Both reference and source samples of Er_6Fe_{23} were found to be single phased with the face-centered-cubic Th_6Mn_{23} structure ($Fm3m$). The Curie temperature of both samples is 493 K. Figure 8 shows the room-temperature spectra of the reference sample and the ^{57}Co-doped source sample. The Mössbauer spectrum of the reference was fitted with four subspectra in the ratio 1:6:8:8 corresponding to the iron occupations of the 4*b*, 24*d*, $32f_1$, and $32f_2$ sites, respectively. More details of fitting are presented in Ref. 33. The solid line in Fig. 8 represents the fit to the data. It is clear from a visual inspection of the source spectrum shown in Fig. 8 that the line at 4.2 mms^{-1} (indicated by an arrow) is greatly reduced in intensity, and therefore Co tends to avoid this site (f_2). The observed cobalt occupations of the four crystallographically inequivalent iron sites are compared to values expected from a random distribution in Fig. 4(c). It is clear that Co favors the f_1 site and avoids the f_2 and *b* sites, while occupying the *d* site essentially at random.

D. $DyFe_3$

Both reference and cobalt-doped samples were confirmed to have the rhombohedral $PuNi_3$ ($R\bar{3}m$) structure by x-ray diffraction. No secondary phases were found in either sample. TGA measurements showed the Curie temperature to be 616 K for both samples. The reference spectrum of $DyFe_3$ in Fig. 9 was fitted with three subspectra in the ratio 1:2:6 corresponding to the iron occupations of the 3*b*, 6*c*, and 18*h* sites, respectively. Since the easy direction of the magnetization lies in the basal plane,[34,35] we have included a further 2:2:2 magnetic subsplitting of the 18*h*-site contributions. van der Kraan *et al.*[35] have concluded from the results of their fitted Mössbauer spectrum that the magnetization lies along the *b* axis at 295 K,but in the basal plane when the temperature is lowered. In this instance the *h* sites should split into two subgroups in the ratio of 2:4 at 295 K, and hence the spectrum should be fitted with four subspectra in the ratio of 1:2:2:4. An attempt to fit this spectrum based on this idea, i.e., assuming *b*-axis magnetization, was unsuccessful. In particular, the fit was unable to reproduce the fine structure appearing on the outermost line at the positive velocity of the spectrum. We believe, therefore, that the easy direction of magnetization lies in the *ab* plane. The final fit to the spectrum is shown as a solid line in Fig. 9. The parameters of the complete fit are given in Table II. The *c* site has the largest hyperfine field in agreement with previous Mössbauer results on $DyFe_3$ (Ref. 25) and this is also consistent with band-structure calculations on YFe_3 (Ref. 36). The source spectrum of $DyFe_3$ is shown in Fig. 9 together with that of the reference. The results of the fit reveal that cobalt preferentially occupies the 3*b* site and avoids the 6*c* site as shown in Fig. 4(d). A previous Mössbauer study on $R(Fe_{1-x}Co_x)_3$, (R =Dy,Y), by Arif, Bunbury, and Bowden[37] showed no preferential occupancies in these systems, but the results of a more recent neutron-diffraction work on $Er(Fe_{1-x}Co_x)_3$ (Ref. 11) are in very good agreement with our results.

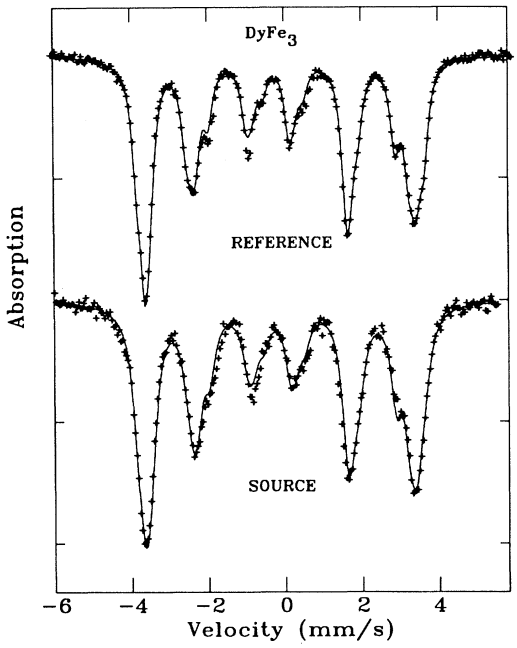

FIG. 9. Mössbauer spectra of the $DyFe_3$ reference and source samples at room temperature. The fits to the data are shown as solid lines. The source spectrum has been inverted.

E. $ThFe_5$

Both x-ray diffraction and TGA measurements showed that after the annealing treatment, both the reference and source samples consisted mainly of the $ThFe_5$ phase with the hexagonal $CaCu_5$ structure ($P6/mmm$). Both samples were found also to contain some Th_2Fe_{17}. The measured values of the Curie temperatures for $ThFe_5$ and Th_2Fe_{17} are 685 K and 302 K, respectively. The Mössbauer spectrum of the reference sample measured at room temperature is shown in Fig. 10(a). The extra lines at the center of the spectrum are due to the secondary phase, Th_2Fe_{17}, whose Mössbauer spectrum is shown in Fig. 10(b). Fortunately, the T_c of Th_2Fe_{17} is near room temperature and much lower than that of $ThFe_5$, allowing us to distinguish the contributions of these two phases in the Mössbauer spectrum. More importantly, the outer lines of the $ThFe_5$ spectrum are well clear of any interference, and thus the subspectra corresponding to the two crystallographically inequivalent iron sites may be identified unambiguously. The reference spectrum was fitted with two subspectra in the ratio 3:2 corresponding to the iron occupations of *g* and *c* sites in the $ThFe_5$ phase and four subspectra associated with the four iron sites of Th_2Fe_{17}, which accounts for ~25% of the total area. Starting values of the hyperfine parameters were taken from the literature.[26,38] As usual, a further 1:1:1 magnetic subsplitting of the *g* site was included to take account of the magnetization being in the basal plane. Fitted parameters of $ThFe_5$ are given in Table II. The results are consistent with those obtained by Gub-

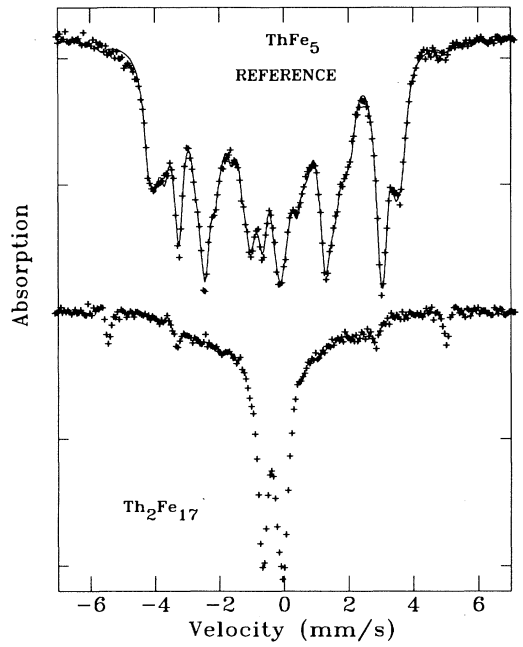

FIG. 10. Mössbauer spectrum for the reference samples of $ThFe_5$ at room temperature. The fit to the data, shown as a solid line, includes a contribution due to Th_2Fe_{17}. The spectrum of a sample of Th_2Fe_{17} at room temperature is also shown in the figure (there is some α-Fe contamination evident).

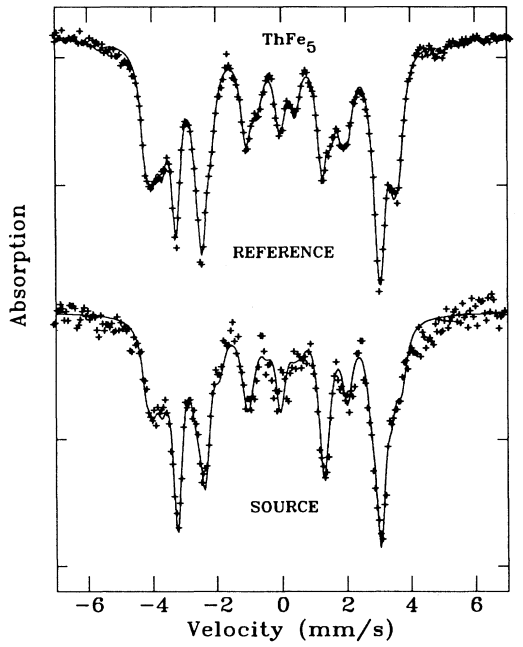

FIG. 11. Mössbauer spectra of the $ThFe_5$ reference and source samples at room temperature. The contributions of the Th_2Fe_{17} impurity phase have been subtracted from both spectra. The fits to the data are shown in solid lines. The source spectrum has been inverted.

bens and van der Kraan.[26,38]

The source spectrum is compared with that of the reference in Fig. 11. To simplify the comparison, the Th_2Fe_{17} contributions (amounting to $\sim 40\%$ in the case of the source and $\sim 25\%$ for the reference sample) were subtracted from the measured spectra. The larger scatter in source spectrum is due to this subtraction. It is quite clear that the intensity of the outermost lines in the source spectrum are reduced, indicating cobalt avoidance of this site ($3g$). The results of the fitted source spectrum confirm that Co, indeed, prefers the c site over the g site in the $ThFe_5$ compound. These results agree very well with that obtained by the neutron-diffraction studies on the $Th(Fe_{1-x}Co_x)_5$ alloys.[7,8]

IV. DISCUSSION

The results of Co-site preferences obtained in this work are summarized in Table III. The table lists the observed Co occupations and site preferences, which are represented by the ratio of observed Co occupation to random occupation. The table also includes the hyperfine field (B_{hf}) or average hyperfine field, where the site exhibits a magnetic subsplitting. It is interesting to note from an inspection of Table III that in each compound, the iron site with the largest hyperfine field is strongly avoided by cobalt; furthermore, the sites that cobalt tends to occupy preferentially are generally those with the smallest hyperfine fields. This correlation between cobalt-site occupation and small hyperfine field (and hence local iron moment) explains the technologically fortunate observation that partially substituting cobalt for iron in a magnet alloy does not lead to the reduction of magnetization predicted by the difference in moments ($2.2\mu_B$ for Fe compared with $1.6\mu_B$ for Co).

A clue to the origin of the observed cobalt-site preferences is provided by their correlation with the iron hyperfine fields. The magnitude of the iron hyperfine field at a given site (which is approximately proportional to the local iron moment) is strongly affected by the local environment of the iron atom, i.e., the type and number of nearest neighbors and the distances to them. It seems likely that similar factors may control the cobalt-site preferences. One measure of a local atomic environment is the Wigner-Seitz cell,[39] which reflects the site symmetry and volume as well as number and type of nearest neighbors. For the Wigner-Seitz cell calculations, the crystallographic data for each compound, given in Table III, are used. We have assumed that all atoms are spherical and that the atomic size is independent on the number and type of nearest neighbors. This latter approximation may not be strictly true as the atomic coordination may have some effect on atomic sizes, as suggested by Pearson.[40] The atomic radii of the elements are taken to be 1.26 Å (Fe), 1.82 Å (Nd), 1.79 Å(Gd), 1.80 Å (Dy), 1.78 Å (Er), 1.80 Å (Th), and 0.98 Å (B), respectively. The resulting nearest-neighbor environments and site volumes for each site in the compounds are summarized in Table III. We have examined the Wigner-Seitz (i.e., Voronoi) polyhedra for all of the transition-metal sites and found that they are essentially regular.

The site volume has been considered as one of the most important factors controlling the site preference in previous studies.[5,17] For example, in Mn-substituted $Er_2Fe_{14}B$, Fuerst, Herbst, and Alson[5] found that the manganese affinity increased with increasing site volume for five of the six transition-metal sites. In studies on cobalt-site preferences, however, the volume consideration has often led to controversy. One reason has been the lack of systematic and reliable data on Co-site preferences. Figure 12 shows the observed Co-site preference plotted against the site volume for all of the compounds studied in this work. It is remarkable that Co-site preference exhibits such clear dependence on the site volume. As can be seen from Fig. 12, Co-site preferences depend linearly on the site volume up to the value of ~ 12.2 Å^3, i.e., the Co affinity decreases with increasing site volume at a rate of ~ 0.9 Å^{-3}. Almost total Co avoidance is found for sites with volumes greater than 12.2 Å^3 with the exception of two sites, where Co actually shows a strong preference. It is interesting to note that the site volume for which Co shows random occupation is ~ 11.6 Å^3 (derived from the straight line fitted to the data points with volumes < 12.2 Å^3 in Fig. 12) close to the volume occupied by iron in bcc α-Fe. In general, the sites with volumes smaller than ~ 11.6 Å^3 are preferred by Co. We therefore conclude that site volume is the dominant parameter controlling the selective substitution of Co for Fe in iron-based intermetallic compounds.

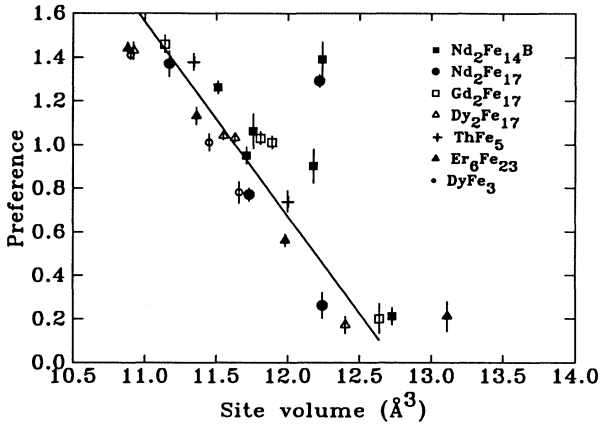

FIG. 12. Site preference (ratio of observed to random occupation) vs site volume for the compounds investigated in this work.

The behavior of Co substitution among the sites with volumes ≥ 12.2 Å^3, however, remains to be explained. As can be seen from Fig. 12, Co strongly prefers two

TABLE III. Summary of observed Co occupations, the site preferences (ratio of observed to random occupation), hyperfine field B_{hf} (or average hyperfine field in the cases where a magnetic subsplitting was used in the fitting) in the various R-Fe compounds studied here. The table also lists site volume and number of nearest neighbors (number of Fe nearest neighbors n_{Fe} and number of rare-earth nearest neighbors n_R) for transition-metal sites in these compounds as determined from Wigner-Seitz analysis.

	Atomic	Cobalt occupations (%)		Site	$\bar{B}_{hf}$	Site		
Compound	site	Random	Observed	preference	(T)	volume (Å^3)	n_{Fe}	n_R
$Nd_2Fe_{14}B$	4*e*	7.14	7.53	1.06	28.8	11.76	9	2
	4*c*	7.14	6.36	0.89	25.6	12.18	8	4
	8j_1	14.3	19.9	1.39	27.9	12.24	9	3
	8j_2	14.3	2.95	0.21	34.3	12.73	12	2
	16k_1	28.6	27.2	0.95	28.8	11.71	10	2
	16k_2	28.6	36.1	1.26	30.6	11.51	10	2
Nd_2Fe_{17}	6*c*	11.8	3.01	0.26	34.7	12.24	13	1
	9*d*	17.6	24.3	1.37	28.2	11.17	10	2
	18*f*	35.3	27.1	0.77	29.7	11.73	11	2
	18*h*	35.3	45.6	1.29	27.2	12.22	9	3
Gd_2Fe_{17}	4*f*	11.8	2.35	0.20	30.2	12.64	13	1
	6*g*	17.6	25.7	1.46	25.0	11.14	10	2
	12*j*	35.3	36.4	1.03	24.8	11.81	11	2
	12*k*	35.3	35.5	1.01	23.3	11.89	9	3
Dy_2Fe_{17}	4*f*	11.8	2.0	0.17	36.1	12.40	13	1
	6*g*	17.6	25.2	1.43	29.9	10.92	10	2
	12*j*	35.3	36.7	1.04	29.5	11.55	11	2
	12*k*	35.3	36.1	1.03	28.7	11.63	9	3
$ThFe_5$	2*c*	40.0	55.5	1.38	19.7	11.34	9	3
	3*g*	60.0	44.5	0.74	22.7	12.00	8	4
Er_6Fe_{23}	4*b*	4.35	0.90	0.21	30.5	13.11	8	6
	24*d*	26.1	29.6	1.13	23.5	11.36	8	4
	32f_1	34.8	50.0	1.44	21.4	10.88	9	3
	32f_2	34.8	19.5	0.56	26.6	11.98	10	3
$DyFe_3$	3*b*	11.1	15.6	1.41	21.4	10.90	6	6
	6*c*	22.2	17.3	0.78	22.5	11.66	9	3
	18*h*	66.7	67.1	1.01	21.3	11.45	7	5

sites, while it completely avoids the other five sites. Such extremely different behavior suggests that besides the site volume effect, there may be other factors controlling Co-site preferences in these iron-based rare-earth compounds. The two Co-preferred sites are the $8j_1$ site in $Nd_3Fe_{14}B$ and the $18h$ site in Nd_2Fe_{17}. The Wigner-Seitz analysis shows that the $8j_1$ and $18h$ sites have identical local atomic environments. Each site has 12 nearest neighbors, of which three are neodymium atoms. The number of rare-earth nearest neighbors in the two sites is substantially larger than that of the other sites in the crystal structures of these two compounds. On the other hand, the five sites, strongly avoided by Co, generally have the largest number of Fe nearest neighbors, with few rare-earth nearest neighbors. It is quite possible, that in these relatively large volume sites, Co substitutions are not controlled solely by the site volume but by a combination of size effects and the chemical affinity between various atoms. van Noort, De Mooij, and Buschow[17] have made an estimate of relative bond strengths between cobalt, neodymium, and iron atoms from the corresponding heats of solution. They find that for Co, the enthalpy of mixing with rare earth is negative and large (-62 kJ mol^{-1} for cobalt in neodymium), while for Fe the value is positive (2 kJ mol^{-1} for iron in neodymium). According to enthalpy considerations, the atoms will tend to have mutual contact as much as possible when the enthalpy of mixing is negative. It follows, therefore, that Co atoms are expected strongly to prefer the $8j_1$ site in $Nd_2Fe_{14}B$ and the $18h$ site in Nd_2Fe_{17}, as is experimentally observed, while Fe atoms will tend to avoid them. It is also quite natural, based on enthalpy considerations, for cobalt not to compete with iron for occupying the other five sites, since there are few rare-earth nearest neighbors around these sites. More importantly, the large volume of these sites is clearly attractive to the iron atoms. Therefore, we believe that the enthalpy effects become increasingly significant in controlling the Co substitutions in Fe-R compounds as the site volume becomes sufficiently large that both Co and Fe atoms can be easily accommodated.

V. CONCLUSIONS

We have shown that the Mössbauer source technique offers a direct and unambiguous way to quantitatively determine cobalt-site preferences in iron-based compounds at extremely low-Co-doping levels (~ 1 ppm). The use of low-Co-content alloys avoids the effects of both changes in the volume of the unit cell, and Co-Co interactions, so that observed site preferences are controlled mainly by local environment effects. Therefore, the results obtained in this work directly reflect the mechanisms controlling the preferential cobalt substitutions at the transition-metal sites in these compounds.

We have performed a systematic study of cobalt-site preferences in iron-based rare-earth intermetallic compounds using the Mössbauer source technique. Our results have given the clearest evidence that cobalt substitutes preferentially among the available sites in all the equilibrium iron-based binary rare-earth intermetallic compounds. The clearest results are the strong Co avoidances of the $8j_2$ site in $Nd_2Fe_{14}B$, $6c(4f)$ sites in R_2Fe_{17} (R =Nd, Gd, Dy), and $4b$ and $32f_2$ sites in Er_6Fe_{23}. The results also show that Co strongly prefers the sites $8j_1$ and $16k_2$ in $Nd_2Fe_{14}B$ $9d$ and $18h$ in Nd_2Fe_{17}, (6g) in both Gd_2Fe_{17} and Dy_2Fe_{17}, $2c$ in $ThFe_5$, $32f_1$ in Er_6Fe_{23}, and $3b$ in $DyFe_3$. All of the sites avoided by cobalt are found to be associated with the largest iron hyperfine field in each compound, while the preferred sites tend to be those with small hyperfine fields; this explains why modest Co additions to iron-based magnet alloys do not generally lead to the expected reduction in magnetization.

We have shown that cobalt-site preferences in iron-based rare-earth compounds are strongly controlled by the local atomic environment based on analysis of the Wigner-Seitz cells. Site volume is the dominant factor controlling preferential cobalt substitutions at iron sites with volumes < 12.2 Å^3. The cobalt preference is found to decrease linearly at a rate of ~ 0.9 Å^{-3} with increasing site volume. In general, cobalt shows a preference for the sites with volume < 11.8 Å^3. As the site volume becomes sufficiently large (≥ 12.2 Å^3), the negative enthalpy of mixing between Co and R plays a significant role in controlling the cobalt-site preferences in combination with the site volume effects. The results show that cobalt strongly avoids the sites with relatively few R nearest-neighbors, while preferring the sites with more R nearest neighbors.

ACKNOWLEDGMENT

This research was supported by grants from the Natural Sciences and Engineering Research Council of Canada, and Fonds pour la Formation de Chercheurs et l'aide à la Recherche, Québec.

*Current address: Department of Physics, Simon Fraser University, Burnaby, British Columbia, Canada V5V 1S6.

[1]J. J. Croat, J. F. Herbst, R. W. Lee, and F. E. Pinkerton, J. Appl. Phys. **55**, 2078 (1984).

[2]M. Sagawa, S. Fujimura, M. Togawa, and Y. Matsuura, J. Appl. Phys. **55**, 2083 (1984).

[3]S. Hirosawa, Y. Matsuura, H. Yamamoto, S. Fujimura, M. Sagawa, and H. Yamauchi, J. Appl. Phys. **59**, 873 (1986).

[4]S. Sinnema, R. J. Radwanski, J. J. M. Franse, D. B. de Mooij, and K. H. J. Buschow, J. Magn. Magn. Mater. **44**, 333 (1984).

[5]C. D. Fuerst, J. F. Herbst, and E. A. Alson, J. Magn. Magn. Mater. **54-57**, 567 (1986).

[6]A. M. van Diepen, K. H. J. Buschow, and J. S. van Wieringen, J. Appl. Phys. **43**, 645 (1972).

[7]J. Laforest and J. S. Shah, IEEE Trans. Magn. **MAG-9**, 217 (1973).

[8]J. B. A. A. Elemans and K. H. J. Buschow, Phys. Status Solidi A **24**, 393 (1974).

[9]R. S. Perkins and P. Fischer, Solid State Commun. **20**, 1010 (1976).

[10]J. F. Herbst, J. J. Croat, R. W. Lee, and W. B. Yelon, J. Appl. Phys. **53**, 250 (1982).
[11]D. E. Tharp, O. A. Pringle, W. J. James, G. K. Marasinghe, G. Long, D. Xie, and W. B. Yelon, J. Less-Common Met. **149**, 363 (1989).
[12]J. F. Herbst and W. B. Yelon, J. Appl. Phys. **60**, 4224 (1986).
[13]D.E. Tharp, Ying-chang Yang, O. A. Pringle, Gary J. Long, and W. J. James, J. Appl. Phys. **61**, 4334 (1987).
[14]Y. D. Zhang, J. I. Budnick, M. Wojcik, E. Potenziani II, A. T. Pedziwiatr, and W. E. Wallace, Phys. Rev. B **36**, 8213 (1987).
[15]J. F. Herbst, J. J. Croat, and W. B. Yelon, J. Appl. Phys. **57**, 4086 (1985).
[16]R. Kumar, W. B. Yelon, and C. D. Fuerst, J. Appl. Phys. **63**, 3725 (1988).
[17]H. M. van Noort, D. B. De Mooij, and K. H. J. Buschow, J. Less Common Met. **115**, 155 (1986).
[18]P. Deppe, M. Rosenberg, S. Hirosawa, and M. Sagawa, J. Appl. Phys. **61**, 4337 (1987).
[19]F. Bolzoni, F. Leccabue, O. Moze, L. Pareti, M. Solzi, and A. Deriu, **61**, 5369 (1987).
[20]J. J. Bara, B. F. Bogacz, and A. Szytula, J. Magn. Magn. Mater. **75**, 293 (1988).
[21]Y. Sano, H. Onodera, H. Yamauchi, and H. Yamamoto, J. Magn. Magn. Mater. **79**, 67 (1989).
[22]M. Matsui, M. Doi, and T. Shimizu, IEEE Trans. Magn. **MAG-23**, 3113 (1987).
[23]H. Honma and H. Ino, IEEE Trans. Magn. **MAG-23**, 3116 (1987).
[24]J. I. Budnick, M. Wojcik, and Y. D. Zhang, in *Hard Magnetic Materials,* Vol. 331 of NATO Advanced Study Institute, Series X: Supermagnets, edited by G. J. Long and F. Grandjean (Kluwer Academic, Boston, 1991), p. 283.
[25]P. Panissod, M. Wojcik, and E. Jedryka, in *Hard Magnetic Materials* (Ref. 24), p. 315.
[26]P. C. M. Gubbens, Ph.D thesis, University of Leiden, 1977.
[27]Y. C. Chang, J. Jiang, and Y. C. Chuang, J. Less-Common Met. **107**, 1 (1985).
[28]D. H. Ryan, Z. Altounian, J. O. Ström-Olsen, and W. B. Muir, Phys. Rev. B **39**, 4730 (1989).
[29]K. H. J. Buschow, Rep. Prog. Phys. **40**, 1179 (1977).
[30]K. H. J. Buschow, J. Appl. Phys. **42**, 3433 (1971).
[31]Supplied carrier free by New England Nuclear Medical Products, DuPont/NEN, N. Billerica, Massachusetts.
[32]L. X. Liao, D. H. Ryan, and Z. Altounian, Rev. Sci. Instrum. (to be published).
[33]L. X. Liao, D. H. Ryan, and Z. Altounian, J. Appl. Phys. **70**, 6143 (1991).
[34]S. K. Arif, D. St. P. Bunbury, G. J. Bowden, and R. K. Day, J. Phys. F **5**, 1048 (1975).
[35]A. M. van der Kraan, J. N. J. van der Velden, J. H. F. van Apeldoorn, P. C. M. Gubbens, and K. H. J. Buschow, Phys. Status Solidi A **35**, 137 (1976).
[36]R. Coehoorn, Phys. Rev. B **39**, 13 072 (1989).
[37]S. K. Arif, D. St. P. Bunbury, and G. J. Bowden, J. Phys. F **5**, 1792 (1975).
[38]P. C. M. Gubbens and A. M. van der Kraan, J. Magn. Magn. Mater. **9**, 349 (1978).
[39]L. Gelato, J. Appl. Cryst. **14**, 141 (1981).
[40]W. B. Pearson, *The Crystal Chemistry and Physics of Metals and Alloys* (Wiley-Interscience, New York, 1972), p. 135.